Supporting Information

Nagy et al. 10.1073/pnas.1305552110

SI Materials and Methods

Computer-Vision Algorithm and Its Validation. The recorded video sequences were analyzed off-line. The position and orientation of all visible colored barcodes were identified in each frame using a dedicated script based on OpenCV, an open-source computer vision library (1). Barcode colors were chosen to minimize interference from the natural coloring of the scene. The first part of the algorithm identified the position of the possible barcode bins using hue-saturation-value color space filtering. This set of bins was analyzed further heuristically to obtain optimal matching with existing barcode definitions for all frames on a possible, smooth trajectory for each barcode. The recognized barcode IDs were added to the original videos for visual inspection of the accuracy and to aid the manual analysis of agonistic interactions.

We tested the accuracy of the automated video tracking against the detailed manual identification of all barcode positions and orientations in all frames of a 12-min video segment, using custom-made software and many hours of manual work. The barcode detection was robust; only 13% remained undetected. For the detected IDs, the match between the automatic and manual recognitions with acceptable error in position (2 pixels = 3.3 cm) and orientation (15°) was 90%. The visual inspection of the other barcode-tagged videos showed acceptable performance as well, especially for the purpose of statistical analysis.

Pecking Order Interaction Coding Protocol. After the automated detection of IDs, we manually scored agonistic interactions to test how our automated dominance analysis methods compared with human observations. For this purpose, we tagged the original video recordings with the identified IDs of birds and used a subtitle editing software to comment on all pairwise interactions with IDs involved, interaction time, duration, and type (i.e., pecking, wing flapping, chasing, retreat, etc.). Again, automatic methods were used to quick-check the manual tagging and categorize interactions into most aggressive, nonaggressive or mutual types.

The format of the subtitles was:

x ID1 *s* ID2,

where *x* denoted the interaction type (see the full list below), ID1 and ID2 denoted the color barcode on the backpacks of birds (three letters, initials of the colors from head to tail), and *s* denoted the interaction type between the birds [i.e., directed (>) or mutual (–)]. In case of directed interactions, ID1 was dominant, ID2 was subordinate.

Identified Interaction Types. The following interaction types were used: p, pecking; w, wing slapping; pm/wm, pecking or wing slapping that misses target; c, chasing; o, obtrusion, pushing; s, scaring away or frightening; f, fighting (could be mutual or clearly one way); d, defense: the attacked one (second bird) tries to defend itself for example by waving its wings or expresses its distress any other way, but not trying to directly attack its attacker; 2*x*, in a fight a clearly defined action (*x* could be w, p, o, etc.) initiated by the attacked bird (second in the interaction); r, retreat: when the attacked one clearly retreats after the action (second bird); g, give up the fight: when the attacker moves away after the action (first bird); i, interesting other event; and n, note: any type of comment.

Definition of Transitivity and Symmetry Indices. In addition to defining simplified dominance scores for each individual, we treat the pairwise interactions as a matrix M, where M_{ij} is the number of interactions [e.g., pecking order (PO), feeding-queuing (FQ), and so forth] initiated by bird i toward bird j. We separate the full interaction matrix into common (C) and dominant (D) parts:

$$M = C + D, \quad \text{where}$$

$$C_{ij} = \min\left(M_{ij}, M_{ji}\right)$$
$$D_{ij} = \max\left(M_{ij} - M_{ji}, 0\right) = M_{ij} - C_{ij}$$

Note that this matrix separation is similar to but slightly different from the standard symmetric/antisymmetric matrix decomposition. Instead of a symmetric part, which is the average of the pairwise interactions, we have a common part that represents the strength of two-way interactions. Similarly, instead of the antisymmetric part, which can contain negative values that are incompatible with some methods, we have a dominant part containing the strength of outgoing interactions, above the level of two-way (common) interactions.

The symmetry index (S) is defined from the C and M matrices as follows:

$$S = \frac{\sum_{i,j,i\neq j} C_{ij}}{\sum_{i,j,i\neq j} M_{ij}}$$

S ranges from 0 to 1; high S values mean that the interactions are overwhelmingly mutual; a small S represent a society where most of the pairwise interactions are dominant in one direction only.

The transitivity index (T) is defined from the D matrix as follows:

$$T = \frac{\sum_{i,j,j>i} D_{ij}}{\sum_{i,j,i\neq j} D_{ij}}$$

Note that T is basically the ratio of the total interactions in the upper triangle of D relative to all of the interactions in D, and thus it is dependent on the order of the rows and columns of the matrix. Therefore, before calculating T, we need to calculate a ranking among the individuals and order the rows accordingly; this is equivalent to the feedback-arc set problem in graph theory. The solution is straightforward if there are no loops and the hierarchy is linear/transitive, and it has multiple equivalent solutions if there are loops or independent subgroups. For a quick close-to-optimal solution, we used a heuristic ranking with the Eades method (2).

T ranges from 0.5 to 1. Higher values correspond to fewer loops in the hierarchy. However, further analysis of the D matrix itself might be needed to interpret T (cluster analysis, careful manual analysis of cases with many loops, etc.). To test the significance of T for a given matrix size, we formed a null distribution by calculating T from the Eades-ordered dominant part (D) of 1 million random matrices (values in the range of 0–100). The T values from this randomization approximate a normal distribution (Fig. S2) with the following fit parameters for matrix sizes 10 and 30 (corresponding to the group sizes in our experiment): adjusted R^2_{10}= 99.87%, $\mu_{10} = 0.79203 \pm 7.3 \times 10^{-5}$, σ_{10}= $0.04908 \pm 7.8 \times 10^{-5}$, adjusted R^2_{30}= 99.91%, $\mu_{30} = 0.68010 \pm 2.2 \times 10^{-5}$, σ_{30}= $0.01676 \pm 2.2 \times 10^{-5}$ (mean ± SE).

Network Representation of Interaction Data and Its Layout. The network representations in the main text and described here (Fig. 3, Fig. S4, and *Inset* in top right corner of Movie S3) were based on the following procedure. The dominant part (see *Definition of Transitivity and Symmetry Indices*) of the interaction matrices [FQ, approach-avoidance (AA), PO, and group flight leadership (GFL)] was calculated. This method is similar to the composition of an antisymmetric matrix and using 0 as a lower limit cutoff. For the network visualization, the cutoff value was actually not 0 but ε, to reduce the effect of noise. In pairs where both individuals fight/dominate/lead the other with almost equal weight ($M_{ij} \approx M_{ji}$, where M represents any of the interaction matrices), the antisymmetric part will be around 0, and the directionality of the interaction will be exposed to a high relative error. To filter these elements, the SD of the matrix was calculated and $\varepsilon = SD(M)/10$ was used as a cutoff. In other words, no edge was drawn between birds i and j if $D_{ij} < \varepsilon$ and $D_{ji} < \varepsilon$. If there was no chain of directed edges from i to j (i.e., no $i \to k \to j$), then i and j were drawn on the same level in the hierarchy.

As shown in *Definition of Transitivity and Symmetry Indices*, these matrices were highly transitive, containing no or very few directed loops (even with 0 as cutoff). To convert the networks with ε cutoff to completely transitive networks, the weakest links in the loops were removed until all of the loops were eliminated. For the FQ networks, four edges were removed for the three groups of 10 (A: two edges, B: zero edges, C: two edges). For the PO networks, one edge was removed from group A. For GFL networks one edge was removed from group B.

In the simultaneous visualization of the different dominance and leadership networks, interaction strength is shown by edge width (Fig. 3 and Fig. S4). For this purpose the networks were normalized by the maximal value (there were no large outliers). The average and SD for the resulting normalized networks (A+B+C) were 0.23 ± 0.20 for FQ, 0.25 ± 0.20 for PO and 0.50 ± 0.22 for GFL.

We used a hierarchical network layout in Fig. 3 *A*–*C* and Fig. S4. These networks were all directed and acyclic (i.e., composed of directed edges and containing no directed loops). We used the hierarchical network visualization of Cytoscape (3), which is in principal based on the Sugiyama method (4). It is a layered graph visualization method in which the vertices of a directed graph are drawn in horizontal rows or layers with the edges generally directed downward. The nodes within each layer are permuted in an attempt to reduce the number of crossings among the edges connecting it to the previous layer. Thus, the horizontal layout contains no information, just supports transparency. The vertical layout contains information about the rank of the nodes. Nodes were added on the same layer if their relative position could not be resolved as either directly or indirectly connected by a directed chain of edges. Our networks were quite densely connected, so in the majority of the cases the rules written above give an unequivocal position for each node. However, in the few cases when a node could be placed on several layers, the highest possible layer was used.

To compare two different networks, we used the 2D hierarchical layout where the vertical positions of the nodes represent the hierarchical layers of one of the networks; the horizontal position of the nodes represents the hierarchical layers of the other network. Edges are placed to maximize transparency.

Dominance Indices. We calculated and compared several dominance indices of the literature on our data, including Kalinoski's frequency of success index, Lindquist's dominance index, the Batchelder-Bershad-Simpson scale score, and de Vries' (modified) (normalized) David's scores (5–8). Because our interaction matrices were highly transitive, the choice of the dominance index was not crucial; that is, the final rankings defined by the different dominance scores were extremely similar (e.g., for FQ interactions the Pearson-correlation between the four scores was over 0.99 for all groups). Therefore, we chose one, the normalized David's score (NormDS) (8), which was simple to calculate and could easily be generalized to matrices with noninteger elements; this was needed in the case of AA and GFL data and for matrices generated from individual scores (e.g., size difference, age difference). In all these cases the normalization factor was not the maximal interaction, as defined originally for matrices with integers, but the total scale of the DS values:

$$NormDS_i = \frac{DS_i - \min_j (DS_j)}{\max_j (DS_j) - \min_j (DS_j)} (n-1),$$

where n is the number of birds in the given group, and DS_i is the original David's score defined as

$$DS_i = w_i(1) + w_i(w_j) - l_i(1) - l_i(l_j), \quad w_i(x) = \sum_{j=1}^{n} x \frac{w_{ij}}{w_{ij} + w_{ji}},$$

$$l_i(x) = \sum_{j=1}^{n} x \left(1 - \frac{w_{ij}}{w_{ij} + w_{ji}}\right).$$

Note that the NormDS scores were calculated from the raw interaction matrices without the Common–Dominant separation. For the matrices generated from individual scores, the NormDS values ranked the individuals in the same order as the original data, with a perfectly linear relation between the two.

Comparing the Interaction Matrices. For each group of 10 (A, B, C) and the group of 30, a two-tailed Pearson correlation was used to compare interaction data from different contexts. Table S1 shows the correlation between NormDS values, as well as an alternative method using the pairwise interaction values (i.e., all matrix elements). For Pearson correlations on pairwise interaction values, we tested significance using the quadratic assignment method [see e.g., Hemelrijk (9)], a type of random permutation procedure. One matrix is permuted by shuffling the individuals into a new order and using this random order in both the rows and the columns. The other matrix is left unchanged. For each permutation, the Pearson correlation between the elements of the two matrices is calculated. The correlation coefficients from 20,000 randomizations formed a null distribution, which we compared with the correlation coefficient between the elements of the two original interaction matrices. In case of positive (negative) correlation, the P value was given as two times the proportion of randomized matrices with a higher (lower) correlation value than the original case.

The comparison described above used the interaction matrix elements as values, which is equivalent to a weighted directed network representation. As an alternative method, we compared the interactions in a way that treats the separated directed (dominant) and undirected (common) parts of the interaction matrices together, within the same framework. Here, the weighted interaction matrices are converted into unweighted mixed graphs containing both directed and undirected connections. For each pair the interaction is characterized by a directed edge represented by 1 (or −1) if the interaction is mostly dominant (or subordinate), an undirected edge represented by 0 if the interaction is best described as mutual, or with no connection if there is no significant interaction between the individuals.

The transformation of the dominant and common parts into directed and undirected edges was as follows: we calculated the average of all values in each matrix and used the averages as lower thresholds. If the dominant part of an interaction was above average, we defined it as a directed edge; if the common part was

above average, we defined it as an undirected edge; otherwise, there was no edge. For the four interaction types (FQ, AA, PO, and GFL), and for all groups, the mixed graphs described above are presented as adjacency matrices in Fig. S5.

Two network similarity measures were used to compare the mixed graphs: the Jaccard Index (10) and the Hamming distance (11). The Jaccard Index is defined as the size of the intersection (the number of pairs that have the same edge in both networks) divided by the size of the union of the sample sets (the number of pairs that have an edge in at least one of the networks):

$$JI(A,B)=\frac{|A\cap B|}{|A\cup B|}.$$

For identical networks, $JI = 1$, whereas values close to 0 indicate low similarity.

The Hamming distance is defined as the number of pairs for which the edges in the two networks are different. Low Hamming distance therefore indicates high similarity between networks. The Hamming distance can be weighted for a given pair, by a factor of 2, when both networks had directed edges but in opposite directions. The weighted Hamming distance gave very similar results to the original Hamming distance, so only the results for the latter are shown.

To test the significance of the similarities, we used the same randomization technique described above. The results of the comparison are presented in Table S2. To test the sensitivity of the results to the chosen threshold for defining edge types, we ran the analysis with thresholds of 120% and 80% of the average. Compared with Table S2, the results from these alternative thresholds only changed the significance of the similarities in 1.4% and 5.6% of cases, respectively, indicating that the results are robust to the choice of threshold. Overall, the comparison using the mixed graph representation gives very similar results to the weighted interaction representation (Table 1, and Tables S1 and S2). This result supports the finding that the hierarchies are different in the dominance and leadership contexts.

Determination of Momentary Leadership. Movie S3 shows momentary leadership roles, based on the directional correlation delay method with a moving time window. At each time step t, $Corr_{ij}$ (τ, t) correlation values were calculated for an interval $[t - 3\text{ s}; t + 3\text{ s}]$, where $Corr_{ij}(\tau,t)=\langle \mathbf{v}_i(t')\cdot\mathbf{v}_j(t'+\tau)\rangle_{t'\in[t-3s;t+3s]}$. For each time step t, the maximal value of the $Corr_{ij}$ (τ, t) correlation function was determined as $\tau^*_{ij}(t)$. The average directional correlation time delay, $\tau^*_i(t)$of bird i at time t was determined by the average $\tau^*_{ij}(t)$ for all j flock members, with the following two conditions: (i) $Corr_{ij}(\tau^*_{ij},t) > Corr_{\min} = 0.9$ and (ii) $v_j(t) > 5$m/s (most probably flying). For further calculations, we only used time steps for which at least three flock members fulfilled the previous two requirements. For each time step t, the degree of momentary leadership was determined by ranking all birds according to their $\tau^*_{ij}(t)$ in decreasing order using fractional ranking. In Movie S3, we label the top six momentary leaders. For these six birds, the size of the dots on both the trajectory and the leadership network is negatively proportional to the momentary leadership rank.

1. Bradski G (2000) The OpenCV Library. *Dr. Dobb's Journal of Software Tools*, Version 2.3.1. Available at http://opencv.willowgarage.com. Accessed August 12, 2011.
2. Eades P, Lin X, Smyth W (1993) A fast and effective heuristic for the feedback arc set problem. *Inf Process Lett* 47(6):319–323.
3. Smoot ME, Ono K, Ruscheinski J, Wang P-L, Ideker T (2011) Cytoscape 2.8: New features for data integration and network visualization. *Bioinformatics* 27(3):431–432.
4. Sugiyama K, Tagawa S, Toda M (1981) Methods for visual understanding of hierarchical system structures. *IEEE Trans Syst Man Cybern* 11(2):109–125.
5. Kalinoski R (1975) Intra- and interspecific aggression in house finches and house sparrows. *Condor* 77(4):375–384.
6. Lindquist WB, Chase ID (2009) Data-based analysis of winner-loser models of hierarchy formation in animals. *Bull Math Biol* 71(3):556–584.
7. Jameson KA, Appleby MC, Freeman LC (1999) Finding an appropriate order for a hierarchy based on probabilistic dominance. *Anim Behav* 57(5):991–998.
8. Bayly KL, Evans CS, Taylor A (2006) Measuring social structure: A comparison of eight dominance indices. *Behav Processes* 73(1):1–12.
9. Hemelrijk C (1990) Models of, and tests for, reciprocity, unidirectionality and other social-interaction patterns at a group level. *Anim Behav* 39(6):1013–1029.
10. Jaccard P (1901) Étude comparative de la distribution florale dans une portion des Alpes et des Jura. *Bull Soc Vaud Sci Nat* 37(142):547–579.
11. Hamming RW (1950) Error detecting and error correcting codes. *Bell Syst Tech J* 29(2): 147–160.

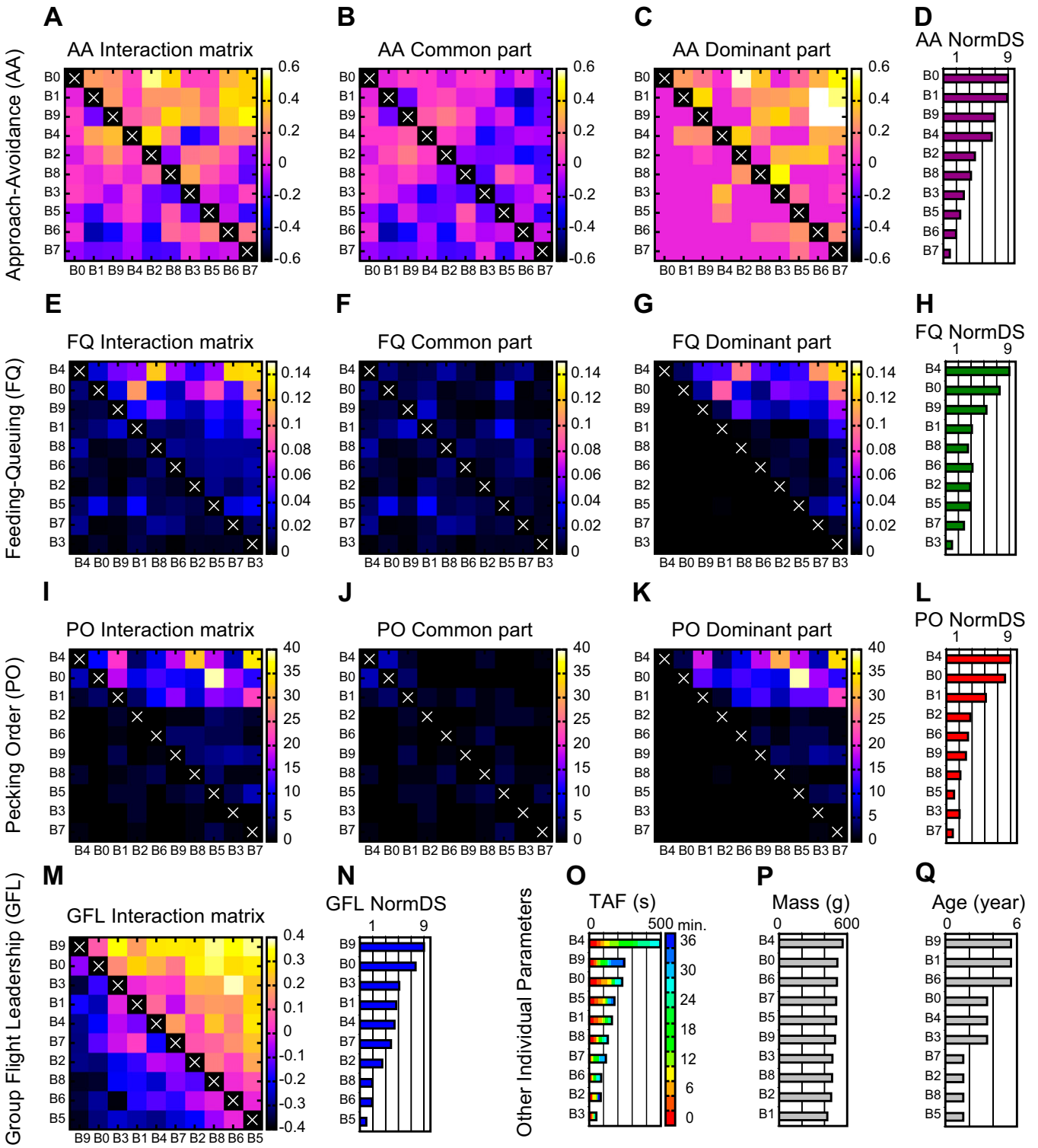

Fig. S1. Interaction matrices and NormDS of group B for AA (*A*–*D*), FQ (*E*–*H*), PO (*I*–*L*), and GFL (*M* and *N*), as well as the individual parameters time-at-feeder (TAF; *O*), body mass (*P*), and age (*Q*). The interaction matrices ("*M*," shown in *A*, *E*, *I*, and *M*) contain all recorded interactions. They were decomposed into a common part ("*C*," shown in *B*, *F*, and *J*) as $C_{ij} = \min(M_{ij}, M_{ji})$ and dominant part ("*D*," shown in *C*, *G*, and *K*) as $D_{ij} = \max(M_{ij} - M_{ji}, 0)$. The NormDS (shown in *D*, *H*, *L*, and *N*) were calculated from antisymmetrized matrices. No decomposition was needed for GFL, because the interaction matrix is antisymmetric by definition. The individuals were ranked separately for each variable, based on the interaction matrix. Therefore, the individuals are shown in the same order across the panels for a variable, but different variables can have different orders. The rankings are the same as used in Fig. 3. In *O*, the color coding shows how much time each bird spent on average at the feeder in each 3-min segment of the feeding period. There was high correlation among all measured body size parameters (wingspan, breast perimeter, mass), so only mass is shown (*P*).

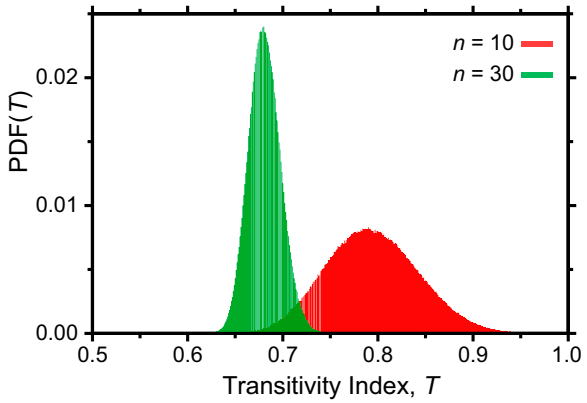

Fig. S2. Probability distribution functions of the Transitivity Index based on 1 million random matrices of size 10 and 30. The transitivity is calculated on the dominant part of the matrices after ordering their rows and columns with Eades-heuristics. The significance of a given *T* value of an arbitrary interaction matrix can be calculated based on the cumulative distribution function of a fitted normal distribution. Note that the significance of a given *T* value strongly depends on matrix size. Bin size on the horizontal axis is 0.001.

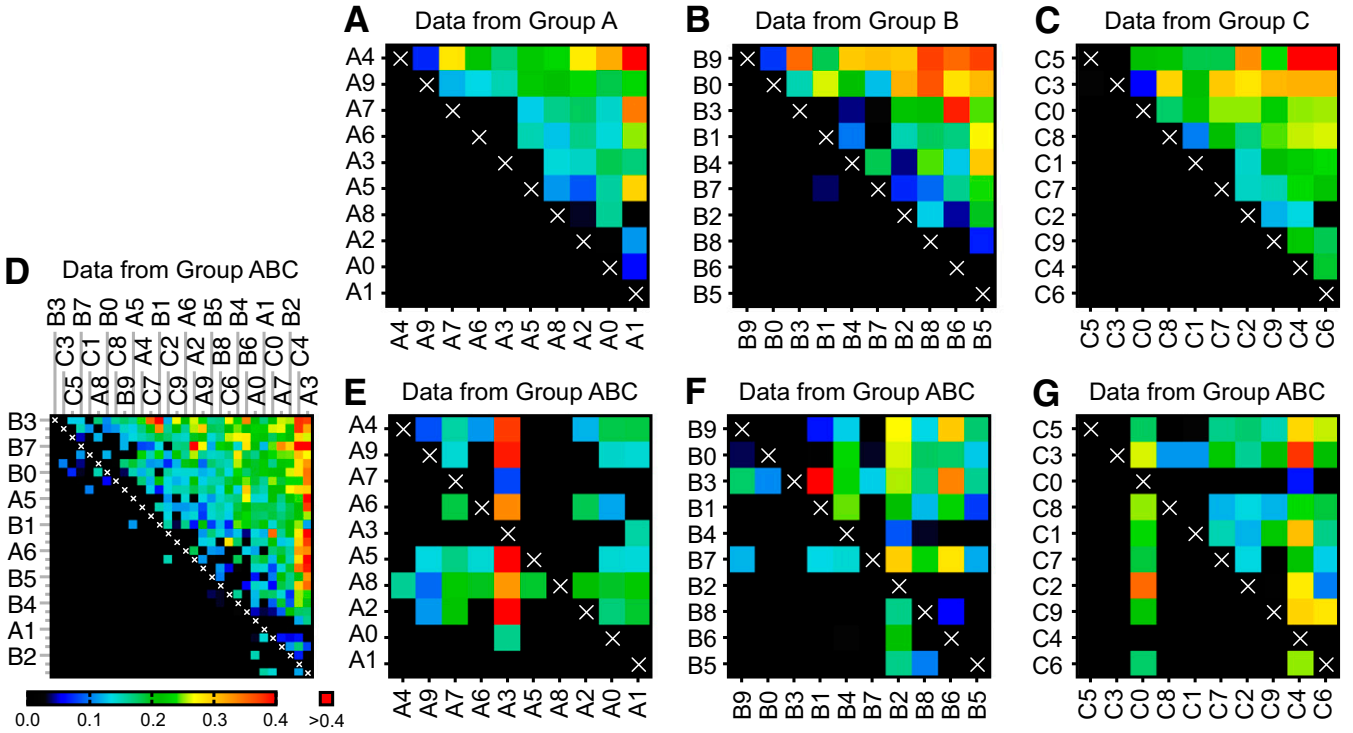

Fig. S3. Interaction matrices of group flight leadership, comparing the groups of 10 and the combined group of 30. Matrices are color-coded according to positive τ^* values (in seconds); that is, the dominant part of the leader–follower interaction divided by 2. In all panels, the more values above the diagonal, the higher the transitivity of the matrix. (*A*–*C*) Interactions measured in the groups of 10. Individuals are ordered according to their NormDS. (*D*) Interactions measured in the combined group of all 30 individuals. Individuals are ordered according to NormDS from the group of 30. (*E*–*G*) To visualize the stability of leader–follower relationships across independent measurements involving 10 and 30 individuals, we plotted on *E*–*G* the same data as in *D* but with individuals in the same order as in *A*–*C* (i.e., using NormDS calculated within groups of 10). The matrices for groups A (in *A* and *E*), B (in *B* and *F*), and C (in *C* and *G*) indicate that most of the leader–follower relationships in the groups of 10 were also detected in the group of 30. The corresponding interaction matrices for FQ are shown in Fig. 2.

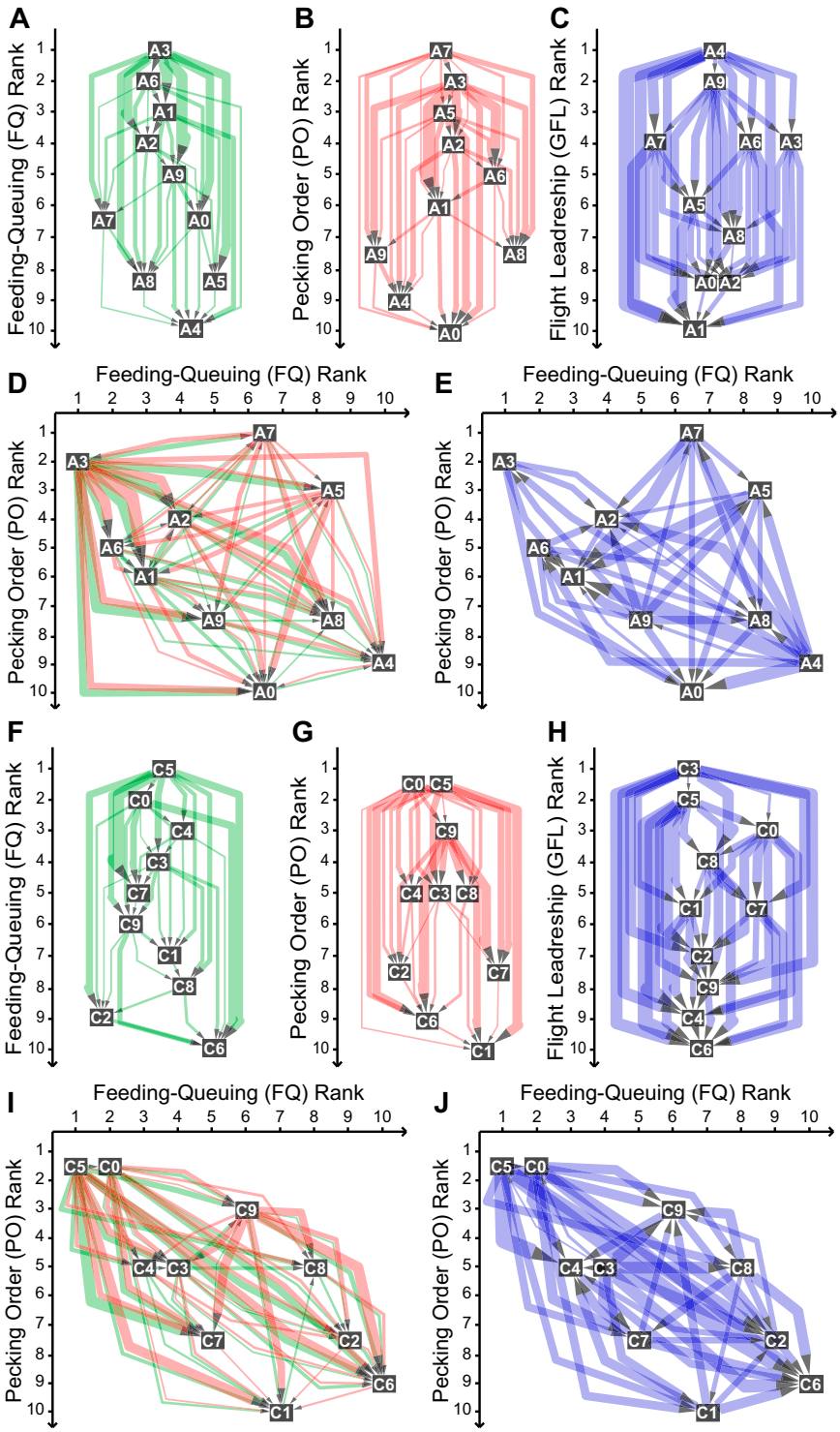

Fig. S4. Dominance and leadership networks for groups A and C. Data for groups A (*A–E*) and C (*F–J*) are presented here using the same types of plots as in Fig. 3. Fig. 3 shows the data for group B.

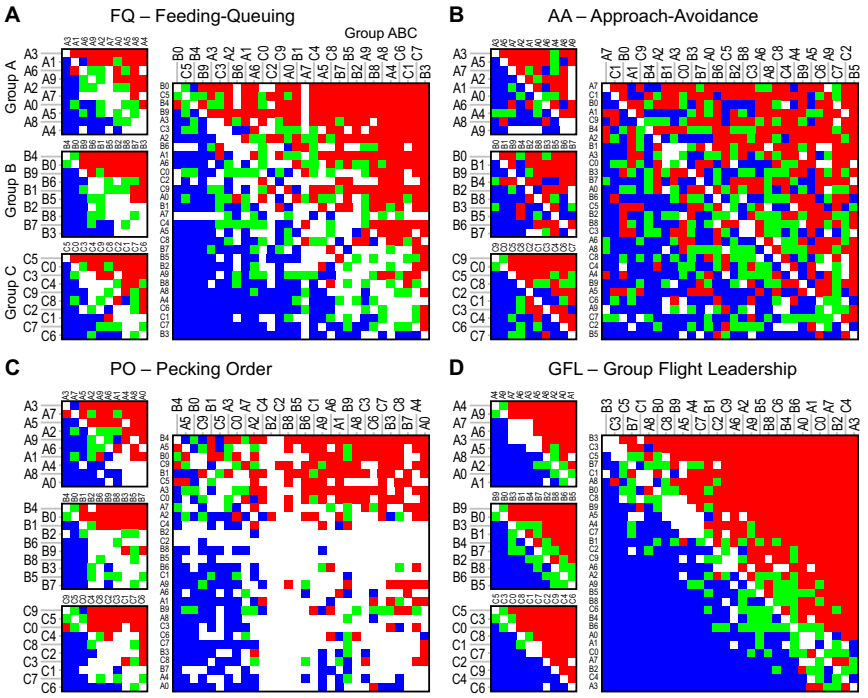

Fig. S5. Adjacency matrices of the mixed graph representation containing both undirected and directed edges for each interaction type (FQ in *A*, AA in *B*, PO in *C*, and GFL in *D*). The 10×10 matrices on the left side of each panel show the data for the groups A, B, and C (from *Top* to *Bottom*, respectively), and the 30×30 matrix contains data for the group of 30. Color indicates the type of the edge: red: directed edge pointing from dominant/leader (in the row) to the subordinate/follower (in the column); blue: directed edge, reverse direction of a red edge; green: undirected edge for mutual interaction; white: no edge. In each matrix the individuals were ordered according to the NormDS scores of that interaction.

Table S1. Comparison of the dominance/leadership indices (*Upper*) and the interaction matrices (*Lower*) for groups A, B, C, and ABC (from left to right)

NormDS - Pearson Correlation Corr. value		Group A (n = 10)							Group B (n = 10)							Group C (n = 10)							Group ABC (n = 30)						
		Dominance			Other Parameters			Lead	Dominance			Other Parameters			Lead	Dominance			Other Parameters			Lead	Dominance			Other Parameters			Lead
		AA	FQ	PO	TAF	Size	Age	GFL	AA	FQ	PO	TAF	Size	Age	GFL	AA	FQ	PO	TAF	Size	Age	GFL	AA	FQ	PO	TAF	Size	Age	GFL
Dominance	AA	X	0.799	0.915	0.564	0.438	0.061	0.020	X	0.655	0.773	0.547	-0.097	-0.476	0.661	X	0.647	0.957	0.471	0.035	0.222	0.340	X	0.258	0.198	0.200	-0.074	0.153	-0.217
	FQ	0.799	X	0.707	0.825	0.546	-0.008	-0.018	0.655	X	0.848	0.891	0.651	-0.258	0.425	0.647	X	0.755	0.676	0.517	-0.391	0.703	0.258	X	0.541	0.678	0.649	-0.270	-0.255
	PO	0.915	0.707	X	0.482	0.327	-0.067	0.153	0.773	0.848	X	0.766	0.374	-0.343	0.420	0.957	0.755	X	0.556	0.252	0.032	0.358	0.198	0.541	X	0.339	0.278	-0.034	-0.236
Other Parameters	TAF	0.564	0.825	0.482	X	0.788	-0.198	-0.266	0.547	0.891	0.766	X	0.643	-0.136	0.294	0.471	0.676	0.556	X	0.549	-0.245	0.729	0.200	0.678	0.339	X	0.562	-0.167	0.089
	Size	0.438	0.546	0.327	0.788	X	-0.072	-0.585	-0.097	0.651	0.374	0.643	X	0.043	0.072	0.035	0.517	0.252	0.549	X	-0.723	0.194	-0.074	0.649	0.278	0.562	X	-0.257	-0.081
	Age	0.061	-0.008	-0.067	-0.198	-0.072	X	-0.364	-0.476	-0.258	-0.343	-0.136	0.043	X	-0.484	0.222	-0.391	0.032	-0.245	-0.723	X	-0.209	0.153	-0.270	-0.034	-0.167	-0.257	X	-0.107
Leadership	GFL	0.020	-0.018	0.153	-0.266	-0.585	-0.364	X	0.661	0.425	0.420	0.294	0.072	-0.484	X	0.340	0.703	0.358	0.729	0.194	-0.209	X	-0.217	-0.255	-0.236	0.089	-0.081	-0.107	X
P-Value		AA	FQ	PO	TAF	Size	Age	GFL	AA	FQ	PO	TAF	Size	Age	GFL	AA	FQ	PO	TAF	Size	Age	GFL	AA	FQ	PO	TAF	Size	Age	GFL
Dominance	AA	X	**0.006**	**<0.001**	0.090	0.206	0.866	0.956	X	**0.040**	**0.009**	0.101	0.790^{-}	0.165^{-}	**0.037**	X	**0.043**	**<0.001**	0.169	0.924	0.537	0.336	X	0.168	0.293	0.289	0.699^{-}	0.420	0.249^{-}
	FQ	**0.006**	X	**0.022**	**0.003**	0.102	0.982^{-}	0.960^{-}	**0.040**	X	**0.002**	**<0.001**	**0.042**	0.472^{-}	0.221	**0.043**	X	**0.012**	**0.032**	0.126	0.264^{-}	**0.023**	0.168	X	**0.002**	**<0.001**	**<0.001**	0.149^{-}	0.175^{-}
	PO	**<0.001**	**0.022**	X	0.159	0.357	0.854^{-}	0.672	**0.009**	**0.002**	X	**0.010**	0.288	0.332^{-}	0.226	**<0.001**	**0.012**	X	0.095	0.482	0.929	0.309	0.293	**0.002**	X	0.067	0.138	0.858^{-}	0.209^{-}
Other Parameters	TAF	0.090	**0.003**	0.159	X	**0.007**	0.583^{-}	0.458^{-}	0.101	**<0.001**	**0.010**	X	**0.045**	0.708^{-}	0.410	0.169	**0.032**	0.095	X	0.101	0.496^{-}	**0.017**	0.289	**<0.001**	0.067	X	**0.001**	0.377^{-}	0.638
	Size	0.206	0.102	0.357	**0.007**	X	0.844^{-}	0.075^{-}	0.790^{-}	**0.042**	0.288	**0.045**	X	0.906	0.843	0.924	0.126	0.482	0.101	X	**0.018**$^{-}$	0.591	0.699	**<0.001**	0.138	**0.001**	X	0.170^{-}	0.670^{-}
	Age	0.866	0.982^{-}	0.854^{-}	0.583^{-}	0.844^{-}	X	0.301^{-}	0.165^{-}	0.472^{-}	0.332^{-}	0.708^{-}	0.906	X	0.157^{-}	0.537	0.264^{-}	0.929	0.496^{-}	**0.018**$^{-}$	X	0.562^{-}	0.420	0.149^{-}	0.858^{-}	0.377^{-}	0.170^{-}	X	0.573^{-}
Leadership	GFL	0.956	0.960^{-}	0.672	0.458^{-}	0.075^{-}	0.301^{-}	X	**0.037**	0.221	0.226	0.410	0.843	0.157^{-}	X	0.336	**0.023**	0.309	**0.017**	0.591	0.562^{-}	X	0.249^{-}	0.175^{-}	0.209^{-}	0.638	0.670^{-}	0.573^{-}	X
Pairwise Interaction - Pearson Corr. Corr. value		AA	FQ	PO	TAF	Size	Age	GFL	AA	FQ	PO	TAF	Size	Age	GFL	AA	FQ	PO	TAF	Size	Age	GFL	AA	FQ	PO	TAF	Size	Age	GFL
Dominance	AA	X	0.536	0.615	0.368	0.286	0.040	-0.007	X	0.417	0.506	0.387	-0.068	-0.336	0.415	X	0.439	0.758	0.380	0.028	0.180	0.234	X	0.196	0.144	0.164	-0.060	0.004	-0.067
	FQ	0.536	X	0.667	0.748	0.495	-0.007	-0.040	0.417	X	0.764	0.840	0.614	-0.243	0.419	0.439	X	0.641	0.607	0.465	-0.351	0.579	0.196	X	0.377	0.602	0.564	-0.244	-0.043
	PO	0.615	0.667	X	0.410	0.278	-0.057	0.149	0.506	0.764	X	0.672	0.327	-0.300	0.367	0.758	0.641	X	0.507	0.230	0.030	0.277	0.144	0.377	X	0.335	0.248	-0.117	-0.116
Other Parameters	TAF	0.368	0.748	0.410	X	0.788	-0.198	-0.289	0.387	0.840	0.672	X	0.643	-0.136	0.281	0.380	0.607	0.507	X	0.549	-0.245	0.690	0.164	0.602	0.335	X	0.540	-0.168	0.070
	Size	0.286	0.495	0.278	0.788	X	-0.072	-0.606	-0.068	0.614	0.327	0.643	X	0.043	0.069	0.028	0.465	0.230	0.549	X	-0.723	0.186	-0.060	0.564	0.248	0.540	X	-0.139	-0.101
	Age	0.040	-0.007	-0.057	-0.198	-0.072	X	-0.357	-0.336	-0.243	-0.300	-0.136	0.043	X	-0.463	0.180	-0.351	0.030	-0.245	-0.723	X	-0.202	0.004	-0.244	-0.117	-0.168	-0.139	X	-0.119
Leadership	GFL	-0.007	-0.040	0.149	-0.289	-0.606	-0.357	X	0.415	0.419	0.367	0.281	0.069	-0.463	X	0.234	0.579	0.277	0.690	0.186	-0.202	X	-0.067	-0.043	-0.116	0.070	-0.101	-0.119	X
P-Value		AA	FQ	PO	TAF	Size	Age	GFL	AA	FQ	PO	TAF	Size	Age	GFL	AA	FQ	PO	TAF	Size	Age	GFL	AA	FQ	PO	TAF	Size	Age	GFL
Dominance	AA	X	0.052	**0.002**	0.112	0.192	0.895	0.855^{-}	X	0.055	**0.004**	0.070	0.786^{-}	0.103^{-}	**0.041**	X	0.070	**<0.001**	0.055	0.897	0.446	0.328	X	**<0.001**	**0.043**	**0.048**	0.580^{-}	0.977	0.338^{-}
	FQ	0.052	X	**0.002**	**<0.001**	0.088	0.973^{-}	0.821^{-}	0.055	X	**<0.001**	**<0.001**	**0.017**	0.400^{-}	**0.049**	0.070	X	**0.002**	**0.013**	0.119	0.205^{-}	**0.015**	**<0.001**	X	**<0.001**	**<0.001**	**<0.001**	0.083^{-}	0.770^{-}
	PO	**0.002**	**0.002**	X	0.128	0.259	0.820^{-}	0.454	**0.004**	**<0.001**	X	**0.010**	0.243	0.275^{-}	0.093	**<0.001**	**0.002**	X	**0.022**	0.422	0.905	0.309	**0.043**	**<0.001**	X	**0.017**	0.062	0.452^{-}	0.267^{-}
Other Parameters	TAF	0.112	**<0.001**	0.128	X	**<0.001**	0.500^{-}	0.260^{-}	0.070	**<0.001**	**0.010**	X	**0.049**	0.717^{-}	0.265	0.055	**0.013**	**0.022**	X	0.065	0.345^{-}	**0.001**	**0.048**	**<0.001**	**0.017**	X	**<0.001**	0.362^{-}	0.605
	Size	0.192	0.088	0.259	**<0.001**	X	X	**0.007**$^{-}$	0.786^{-}	**0.017**	0.243	**0.049**	X	X	0.759	0.897	0.119	0.422	0.065	X	X	0.500	0.580^{-}	**<0.001**	0.062	**<0.001**	X	X	0.498^{-}
	Age	0.895	0.973^{-}	0.820^{-}	0.500^{-}	X	X	0.198^{-}	0.103^{-}	0.400^{-}	0.275^{-}	0.717^{-}	X	X	0.071^{-}	0.446	0.205^{-}	0.905	0.345^{-}	X	X	0.445^{-}	0.977	0.083^{-}	0.452^{-}	0.362^{-}	X	X	0.447^{-}
Leadership	GFL	0.855^{-}	0.821^{-}	0.454	0.260^{-}	**0.007**$^{-}$	0.198^{-}	X	**0.041**	**0.049**	0.093	0.265	0.759	0.071^{-}	X	0.328	**0.015**	0.309	**0.001**	0.500	0.445^{-}	X	0.338^{-}	0.770^{-}	0.267^{-}	0.605	0.498^{-}	0.447^{-}	X
		Group A (n = 10)							Group B (n = 10)							Group C (n = 10)							Group ABC (n = 30)						

For more information, see *Comparing the Interaction Matrices*. Cells that contain significant correlations ($P < 0.05$) are in bold. Correlation values are color-coded on a continuous scale from blue through green to red, with values close to −1 in blue, those close to 0 in green, and those close to 1 in red. *P* values in white show nonsignificant correlations; those on a red color-scale show significant positive correlations, and those on a blue color-scale show significant negative correlations. A superscript "−" shows a *P* value where the correlation coefficient is negative. An "x" indicates cells where correlations are not applicable.

Table S2. Comparison of the dominance/leadership networks using an unweighted (binary) mixed graph representation containing mutual and directed connections

Jaccard Index (*JI*)

		Group A (*n* = 10)					Group B (*n* = 10)					Group C (*n* = 10)					Group ABC (*n* = 30)				
		Dominance			Leadership		Dominance			Leadership		Dominance			Leadership		Dominance			Leadership	
JI		AA	FQ	PO	GFL	GFL R	AA	FQ	PO	GFL	GFL R	AA	FQ	PO	GFL	GFL R	AA	FQ	PO	GFL	GFL R
Dominance	AA	X	0.34	0.45	0.29	0.29	X	0.50	0.51	0.51	0.24	X	0.42	0.51	0.49	0.29	X	0.30	0.21	0.29	0.30
	FQ	0.34	X	0.48	0.32	0.27	0.50	X	0.55	0.44	0.18	0.42	X	0.50	0.52	0.09	0.30	X	0.29	0.23	0.28
	PO	0.45	0.48	X	0.29	0.18	0.51	0.55	X	0.40	0.11	0.51	0.50	X	0.41	0.14	0.21	0.29	X	0.15	0.18
Leadership	GFL	0.29	0.32	0.29	X	X	0.51	0.44	0.40	X	X	0.49	0.52	0.41	X	X	0.29	0.23	0.15	X	X

***P*-value**

		AA	FQ	PO	GFL	GFL R	AA	FQ	PO	GFL	GFL R	AA	FQ	PO	GFL	GFL R	AA	FQ	PO	GFL	GFL R
Dominance	AA	X	0.150	**0.006**	0.740	0.582	X	**0.003**	**<0.001**	0.050	0.557	X	0.122	**0.010**	0.109	0.850	X	**0.002**	**0.001**	0.703	0.601
	FQ	0.150	X	**<0.001**	0.160	0.317	**0.003**	X	**0.001**	0.093	0.773	0.122	X	**0.002**	**0.001**	0.990	**0.002**	X	**<0.001**	0.790	0.423
	PO	**0.006**	**<0.001**	X	0.801	0.990	**<0.001**	**0.001**	X	0.076	0.975	**0.010**	**0.002**	X	0.127	0.981	**0.001**	**<0.001**	X	0.923	0.456
Leadership	GFL	0.740	0.160	0.801	X	X	0.050	0.093	0.076	X	X	0.109	**0.001**	0.127	X	X	0.703	0.790	0.923	X	X

Hamming Distance (*HD*)

HD		AA	FQ	PO	GFL	GFL R	AA	FQ	PO	GFL	GFL R	AA	FQ	PO	GFL	GFL R	AA	FQ	PO	GFL	GFL R
Dominance	AA	X	58	48	64	64	X	44	42	44	68	X	52	44	46	64	X	594	650	616	604
	FQ	58	X	44	60	64	44	X	36	50	74	52	X	40	42	80	594	X	506	658	616
	PO	48	44	X	64	74	42	36	X	54	80	44	40	X	52	76	650	506	X	726	694
Leadership	GFL	64	60	64	X	X	44	50	54	X	X	46	42	52	X	X	616	658	726	X	X

***P*-value**

		AA	FQ	PO	GFL	GFL R	AA	FQ	PO	GFL	GFL R	AA	FQ	PO	GFL	GFL R	AA	FQ	PO	GFL	GFL R
Dominance	AA	X	0.171	**0.009**	0.772	0.640	X	**0.004**	**<0.001**	0.050	0.557	X	0.122	**0.010**	0.109	0.850	X	**0.006**	**0.001**	0.734	0.641
	FQ	0.171	X	**<0.001**	0.201	0.374	**0.004**	X	**0.003**	0.093	0.773	0.122	X	**0.001**	**0.001**	0.985	**0.006**	X	**<0.001**	0.839	0.496
	PO	**0.009**	**<0.001**	X	0.862	0.995	**<0.001**	**0.003**	X	0.076	0.975	**0.010**	**0.001**	X	0.140	0.976	**0.001**	**<0.001**	X	0.989	0.763
Leadership	GFL	0.772	0.201	0.862	X	X	0.050	0.093	0.076	X	X	0.109	**0.001**	0.140	X	X	0.734	0.839	0.989	X	X

Group A (*n* = 10)	Group B (*n* = 10)	Group C (*n* = 10)	Group ABC (*n* = 30)

Results from two network similarity measures are shown: the Jaccard Index (JI, *Upper*) and Hamming distance (HD, *Lower*) for groups A, B, C, and ABC (from left to right). For details see *Comparing the Interaction Matrices*. *JI* and *HD* values are color-coded red for more similar networks, green for less similar networks. In the *P* value tables, cells that contain significant correlations ($P < 0.05$) are in bold, with deeper reds showing stronger correlations. To check for possible anticorrelation between dominance and leadership, we also calculated the Jaccard Index and the Hamming distance with the directed GFL interactions reversed (GFL R column). No such anticorrelation was found.

Table S3. Detailed information about all of the automatic and manual methods used in our analysis

Type and abbreviation	Method	General description	Specific descriptions and comments	Applicability of method
Dominance				
AA	Approach-Avoidance	Automated scoring based on correlations between relative position and direction of motion	Autonomous identification of individual position on video recordings	Any global or local position data (e.g., GPS, motion tracker)
FQ	Feeding-Queuing	Automated scoring based on position to each other relative to the feeder		Proximity measurement from each other and from feeder, or any global or local position data (e.g., GPS, RFID, motion tracker, IR sensor, etc.)
PO	Pecking Order	Manual scoring of social interactions	Computer-aided manual identification of pecking, fighting and chasing actions (pecking, wing slapping, retreat events, etc.) on video recordings	
Other parameters				
TAF	Time-at-Feeder: Time spend with access to food	Automated scoring based on proximity to the feeder	Autonomous identification of individual position on video recordings	Proximity to feeder, or any global or local position data (e.g., GPS, motion tracker, IR sensor, ultrasonic sensor, laser proximity sensor, etc.)
Size	Body size measurements	Body mass (g) Breast size (cm) Wingspan (cm)	Biometric measurements taken several times over the experimental period	
Age	Age	Time since hatched (y)		
Leadership				
GFL	Group Flight Leadership	Directional correlation delay method on flight trajectory	Calculated from high-resolution GPS track logs	Any global or local position data (e.g., GPS, motion tracker)
	Front-Rear Position in Flock	Position (from front to rear) in flock relative to the direction of motion		Any global or local position data (e.g., GPS, motion tracker). Also could be calculated from directed proximity and distance)

The last column describes the requirements of the methods and their applicability for analyzing data from other study systems. IF, infrared; RFID, radio-frequency ID.

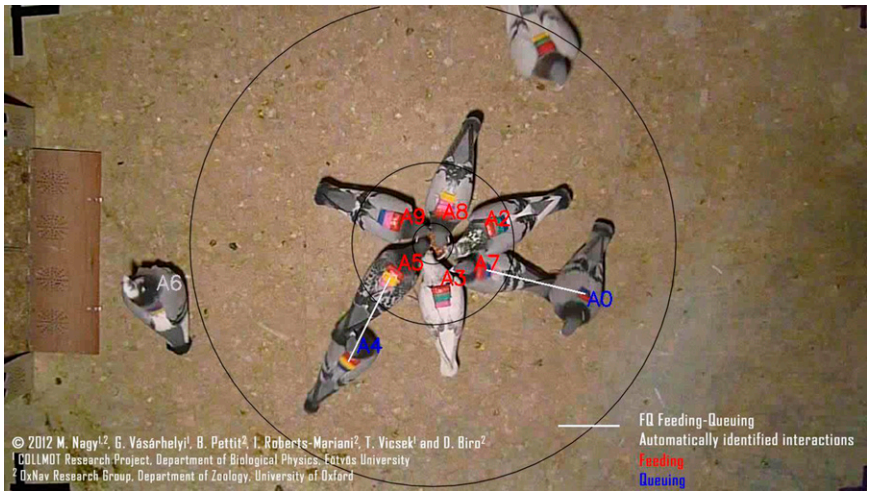

Movie S1. Video of a feeding experiment of 10 pigeons (group A) including an overlay of FQ interactions. The concentric circles indicate the outer boundaries of the feeding and queuing ranges. Feeding birds are marked with red IDs, queuing with blue. White lines show FQ interactions.

Movie S1

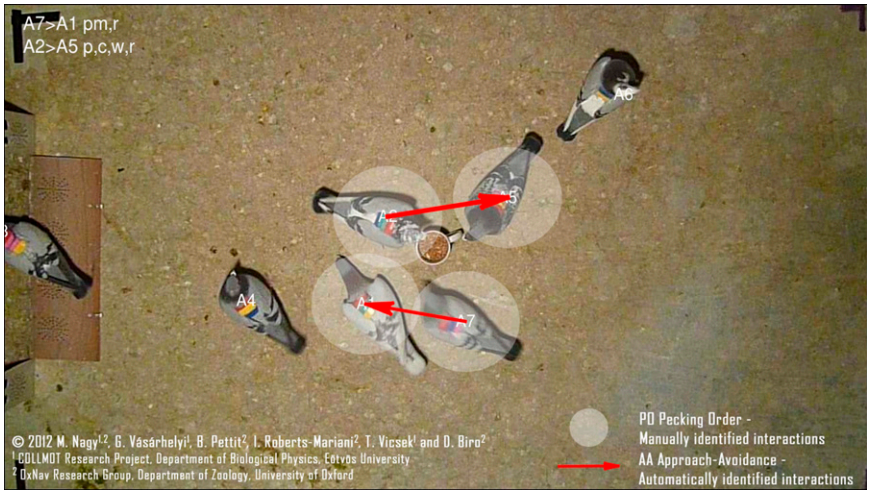

Movie S2. Video of a feeding experiment of 10 pigeons (group A) including an overlay of PO and AA interactions. White spotlights indicate manually identified PO interactions, coded in the top left corner (see *Materials and Methods*). Red arrows indicate AA interactions. For this purpose, AA_{ij} was averaged over a 0.5-s time window. An AA interaction is indicated with an arrow at time t, pointing from bird i (the approaching bird) toward bird j (the one that avoids the approach). To more clearly illustrate the most relevant interactions, we only display arrows where $AA_{ij}(t) \geq 0.8$, $AA_{ji}(t) \leq -0.5$, and $d_{ij} \leq 30$ cm.

Movie S2

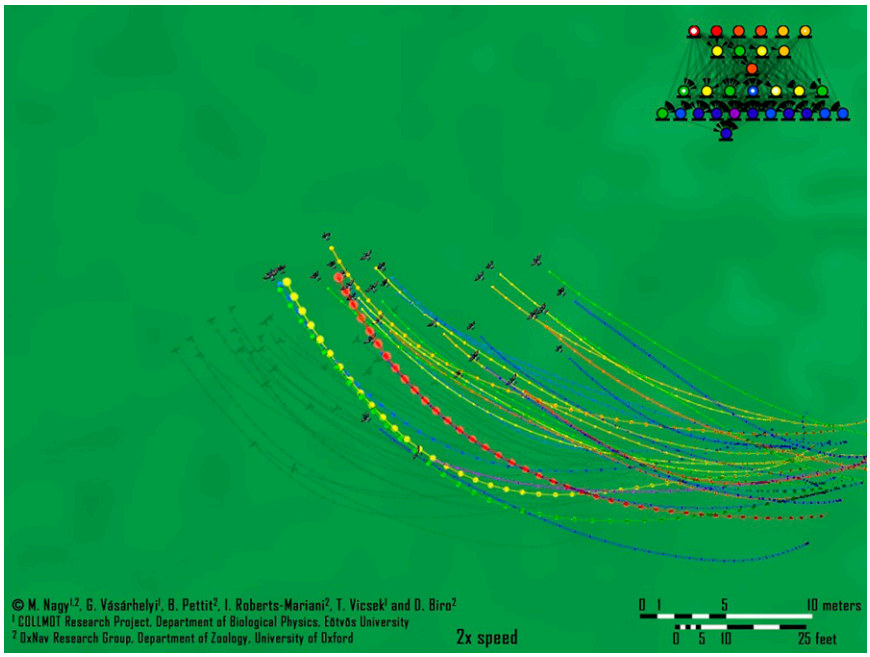

Movie S3. Animation showing 80 s of free flight by 30 pigeons, all equipped with GPS. Video speed is two-times real speed. Individuals are colored according to their ranks in the hierarchy (*Top Right*), determined by pairwise directional correlation delay times for the whole flight. Colors near the red end of the spectrum indicate higher leadership on average. The top six momentary leaders (*SI Materials and Methods*) are indicated by larger dots on the trajectories and white dots on the hierarchy network. The white bars under nodes in the network show the amount of time individuals were among the top six birds.

Movie S3